Research Square

Preprints are preliminary reports that have not undergone peer review.
They should not be considered conclusive, used to inform clinical practice,
or referenced by the media as validated information.

Evolution of Hawking mass under hypersurface-restricted expanding flows

Hollis Williams

holliswilliams@hotmail.co.uk

Okinawa Institute of Science and Technology Graduate University

Research Article

Keywords:

Posted Date: March 16th, 2026

DOI: https://doi.org/10.21203/rs.3.rs-9073165/v1

License: This work is licensed under a Creative Commons Attribution 4.0 International License.
Read Full License

Additional Declarations: No competing interests reported.

Evolution of Hawking mass under hypersurface-restricted expanding flows

Hollis Williams[a,1,*]

[a] *Theoretical Sciences Visiting Program, Okinawa Institute of Science and Technology Graduate University, Onna-son, Okinawa 904-0495, Japan*

Abstract: We present a numerical study of the evolution of the Hawking mass for closed nonspherical surfaces evolved under a class of expanding flows in Minkowski spacetime. Although formal monotonicity of the Hawking mass under smooth inverse mean curvature flow is well established in the Riemannian setting, comparatively little is known about the robustness of this behavior in discrete numerical implementations applied to explicitly embedded surfaces away from exact symmetry. We consider surfaces defined by small spherical harmonic perturbations of a round sphere and evolve them under an in-slice, time-flat flow analogous to inverse mean curvature flow. We examine the behaviour of the Hawking mass under the flow and find that monotonicity persists for a class of nonspherical perturbations and is robust under variations in perturbation amplitude and angular frequency. We also identify regimes in which numerical instabilities arise, highlighting practical challenges associated with extending such flows beyond simple symmetry assumptions. These results provide a concrete computational testbed for future investigations of uniformly expanding flows and quasi-local mass in more general spacetime settings.

1. Introduction

Quasi-local notions of mass in general relativity play a central role in understanding the distribution of energy in spacetimes, since they provide a way to associate an energy content to a spacelike 2-surface using its intrinsic and extrinsic geometry [1, 2, 3, 4, 5, 6, 7]. Amongst the various proposed definitions, the Hawking mass has attracted interest due to its simple geometric definition and its close connection to the Penrose inequality and gravitational collapse [8, 9, 10]. A major advantage of the Hawking mass is its desirable properties under geometric flows: formal monotonicity of the mass under inverse mean curvature flow (IMCF) was a key ingredient in the first proof of the Riemannian Penrose inequality [11, 12]. Uniformly expanding flows (UEFs) extend this idea to spacetime by prescribing an evolution of surfaces with constant expansion, allowing both spacelike and timelike components of the mean curvature vector to contribute [13]. In this framework, the notion of a time-flat surface was introduced and variational formulas have been derived showing that the Hawking mass is formally nondecreasing along spacelike UEFs under suitable conditions [14]. These flows are a natural way to investigate monotonicity properties of quasi-local masses and may be considered as a generalization of the IMCF.

However, these monotonicity results are proved under the assumption that a smooth flow exists: no general existence theory is known, and no analysis has been performed for surfaces deviating from perfect symmetry, with less known about the stability of this behaviour. In particular, no numerical or perturbative studies have tested the robustness of monotonicity under non-spherical deformations. On the formal side, a full existence theory for general spacelike UEFs remains challenging due to the forward-backward parabolic nature of the associated system of PDEs. In this work, we take a complementary, computational approach. Rather than attempting to construct the most general uniformly expanding flow in a spacetime, we focus on a physically natural and mathematically well-defined subclass: in-slice, time-flat flows of closed spacelike 2-surfaces. When the surfaces lie in a fixed spacelike hypersurface and satisfy the time-flat condition, the uniformly expanding flow condition reduces to IMCF within the slice. This specialization allows for explicit calculations and allows us to evolve a perturbed surface numerically under a UEF and track the evolution of the Hawking mass, providing evidence that monotonicity persists beyond an idealized setting.

The simplest and most natural spacetime which we may consider in this setting is a perturbation of a spherical surface in Minkowski space. Minkowski space appears as the unique zero-mass configuration in general

*Corresponding author. Email: holliswilliams@hotmail.co.uk

relativity with perturbations necessarily increasing the total energy, a fact which underlies the original spinor-based proof of the positive energy theorem [15, 16]. Proofs of this theorem first appeared for small perturbations of Minkowski spacetime, clarifying the role that flat spacetime should play in the general result [17, 18]. For quasi-local masses, we might also expect failures of positivity or monotonicity to first manifest for non-spherical perturbations of flat space. Consequently, verifying monotonicity for small deviations from spherical symmetry in Minkowski spacetime constitutes an essential consistency check for UEFs and their suitability as physical diagnostics. We therefore expect that the behavior of the Hawking mass under perturbations of round spheres in Minkowski space provides a sensitive probe of both rigidity and stability.

Using a spherical harmonic expansion to parametrize nonspherical perturbations of a sphere evaluated on a finite (θ, ϕ) grid, we compute the Hawking mass along the in-slice flow and examine its sensitivity to perturbation amplitude, angular structure, and numerical resolution. This provides direct evidence that the formal monotonicity results for uniformly expanding flows correspond to stable behavior in concrete geometric evolutions, whilst also identifying regimes in which numerical or geometric instabilities may arise. By restricting attention to time-flat, in-slice flows, we obtain a controlled setting in which analytic expectations can be directly compared with numerical results. This serves as a necessary first step toward more general spacetime evolutions and provides new insight into the practical behavior of quasi-local mass under geometrically motivated flows. To our knowledge, such numerical investigations of Hawking mass monotonicity under perturbed flows have not previously been carried out. To parametrise perturbations of the surface geometry, we consider expansions into spherical harmonics. This is a standard technique in perturbative and numerical relativity, where spherical and spin-weighted spherical harmonic decompositions are used to isolate angular modes and achieve spectral convergence [19, 20]. Representations based on spherical harmonics are also widely used in numerical studies of gravitational perturbations and wave extraction [21, 22, 23, 24]. In the present study, restricting to low-order harmonic modes allows us to probe controlled deviations from spherical symmetry while retaining a clear interpretation of the resulting geometric and physical quantities. Moreover, expressing perturbations in an orthonormal harmonic basis enables a systematic assessment of how individual angular modes influence the evolution of the Hawking mass, providing a transparent way to test the robustness of monotonicity under non-spherical deformations when the Hawking mass of the perturbed surface is evolved under an in-slice, time-flat flow. This provides a first numerical confirmation that small perturbations do not violate monotonicity, and establishes a practical framework for future extensions to black hole spacetimes and the full UEF.

The article is structured as follows. In Section 2, we provide background and definitions for the Hawking mass, uniformly expanding flows, time-flat surfaces, and in-slice flows. In Section 3, we outline the numerical framework and method which we use. In Section 4, we provide validation of our methods in the case where there is no flow. In Section 5, we present our numerical results for nonspherical initial data, examining evolution and monotonicity of the Hawking mass under in-slice IMCF-type flow and quantifying robustness of the monotonicity with respect to angular structure and amplitude of the perturbation. We finish with conclusions and future directions in Section 6.

2. Background

2.1. Hawking mass

Let Σ be a smooth, closed, spacelike two-surface embedded in a four-dimensional spacetime $(\mathcal{M}, g)$. Denote by $|\Sigma|$ the area of Σ, and by $\vec{H}$ its mean curvature vector, defined as the trace of the second fundamental form with respect to the induced metric on Σ. The Hawking mass m_H is defined to be

$$m_H(\Sigma) = \sqrt{\frac{|\Sigma|}{16\pi}} \left(1 - \frac{1}{16\pi} \int_\Sigma \langle \vec{H}, \vec{H} \rangle \, dA\right), \tag{1}$$

where dA is the area element induced on Σ. It can be checked with standard calculations that $m_H = 0$ in the case of a round sphere in Minkowski spacetime and that $m_H = m$ for a round sphere in Schwarzschild spacetime with mass m. To explore the behavior of the Hawking mass under small deformations of a spherically symmetric surface, we consider perturbations of a round sphere in the chosen time-symmetric slice. We parametrize the perturbed surface as a radial graph over the sphere:

$$r(\theta, \phi) = R_0[1 + \epsilon Y_{lm}(\theta, \phi)], \quad \epsilon << 1, \tag{2}$$

where R_0 is the radius of the sphere, ϵ is a small dimensionless parameter, and $Y_{lm}(\theta, \phi)$ are spherical harmonics. This representation allows us to study the perturbation analytically mode by mode and is also the starting point

for the analytic calculation of the Hawking mass m_H at time $t = 0$ whose evolution under the flow will be studied numerically.

To calculate the Hawking mass at $t = 0$ for a perturbed sphere in Minkowski spacetime $m_H^M(t = 0)$, one may work in the constant t slice of Minkowski with spherical coordinates (r, θ, ϕ) and expand to first order in ϵ. For a radial graph, the induced metric g_{AB} is

$$g_{AB} = r^2\Omega_{AB} + r_A r_B, \tag{3}$$

where Ω_{AB} is the unit sphere metric and $r_A = \partial_A r$. Since the integral of Y_{lm} over the two-sphere S^2 vanishes for $l \geq 1$, we have

$$dA = r^2 \sin\theta \, d\theta \, d\phi + \mathcal{O}(\epsilon^2), \tag{4}$$

$$|\Sigma| = 4\pi R_0^2 + \mathcal{O}(\epsilon^2). \tag{5}$$

Using the expansion

$$H = \frac{2}{r} - \frac{1}{r^2}\Delta_{S^2} r + \mathcal{O}(|\nabla r|^2), \tag{6}$$

we then have

$$H = \frac{2}{R_0} + \epsilon\left(\frac{l(l+1) - 2}{R_0}\right) Y(\theta, \phi) + \mathcal{O}(\epsilon^2), \tag{7}$$

hence the mean curvature has a linear correction which is proportional to the spherical harmonics. Carrying out the surface integral, we then arrive at

$$m_H^M(t = 0) = \mathcal{O}(\epsilon^2). \tag{8}$$

Performing the analogous calculations for a perturbed sphere in Schwarzschild spacetime with the usual time-symmetric slice

$$ds^2 = \left(1 - \frac{2m}{r}\right)^{-1} dr^2 + r^2 d\Omega^2, \tag{9}$$

we one can also check as expected that

$$m_H^S(t = 0) = m + \mathcal{O}(\epsilon^2). \tag{10}$$

This result for the corrected Hawking mass provides an analytic baseline for comparison with numerical calculations of its evolution under the chosen flow.

2.2. Uniformly expanding flows

Assume that $\vec{H}$ is spacelike, so that its magnitude

$$|\vec{H}| = \sqrt{\langle \vec{H}, \vec{H} \rangle} \tag{11}$$

is well defined. A one-parameter family of surfaces $\{\Sigma_\lambda\}$ is said to evolve by a UEF if the flow vector field $\vec{\xi}$ normal to Σ_λ satisfies

$$\vec{\xi} = \frac{\vec{H}}{|\vec{H}|^2}, \tag{12}$$

or, more generally, if the expansion of the surface along $\vec{\xi}$ is constant on each leaf of the flow. In the Riemannian setting, this reduces to IMCF, where the normal speed is given by the reciprocal of the mean curvature scalar. In spacetime, UEFs generalize IMCF by allowing both spacelike and timelike components of the normal evolution, whilst preserving uniform control of the surface expansion.

2.3. Time-flat surfaces

Let $\{\nu_1, \nu_2\}$ be a local orthonormal frame of the normal bundle $N\Sigma$, with ν_1 chosen to be proportional to the mean curvature vector $\vec{H}$. The normal connection one-form α_H associated with $\vec{H}$ is defined by

$$\alpha_H(X) = \langle \nabla_X \nu_1, \nu_2 \rangle , \qquad X \in T\Sigma. \tag{13}$$

A spacelike two-surface Σ is said to be time-flat if

$$\alpha_H = 0. \tag{14}$$

Geometrically, this condition implies that the mean curvature vector does not rotate within the normal bundle and that the normal evolution of the surface does not twist. This is the condition under which additional normal-bundle contributions to the evolution of the Hawking mass vanish, motivating its use in numerical investigations of monotonicity.

2.4. In-slice flows

Let H denote the mean curvature scalar of Σ computed with respect to h, and let ν be the outward unit normal to Σ within M. An in-slice inverse mean curvature flow is defined by the evolution equation

$$\frac{\partial x}{\partial \lambda} = \frac{1}{H}\,\nu, \tag{15}$$

where $x(\lambda)$ denotes the embedding of the evolving surface Σ_λ into M, and λ is a flow parameter labeling the leaves of the evolution. Although the evolution is confined to a fixed spacelike hypersurface, the Hawking mass is computed using the spacetime mean curvature vector. This setting should be viewed not as a replacement for the full spacetime UEF equations, but as a controlled restriction designed to probe the stability and robustness of Hawking mass monotonicity under explicit geometric evolution. The construction may be viewed as a hypersurface-restricted realization of a UEF, chosen here for numerical tractability whilst retaining the geometric features underlying Hawking mass monotonicity.

3. Numerical framework

As explained in Section 2, each evolving surface is represented as a radial graph over the unit sphere. This representation is well suited to small nonspherical perturbations and allows efficient computation of geometric quantities on S^2. In the in-slice setting considered here, the mean curvature scalar H is approximated using the standard expansion for a radial graph in Euclidean space

$$H = \frac{2}{r} - \frac{1}{r^2}\,\Delta_{S^2} r + \mathcal{O}(|\nabla r|^2), \tag{16}$$

where Δ_{S^2} denotes the Laplacian on the unit sphere. This approximation is sufficient for the perturbative regime explored in this work and was validated against analytic results for round spheres and small deformations.

The surface is evolved according to an in-slice IMCF

$$\frac{\partial r}{\partial \lambda} = \frac{1}{H}. \tag{17}$$

The flow was integrated using an explicit Euler scheme with fixed time step Δt, chosen sufficiently small to ensure numerical stability and results were verified to be insensitive to further time step refinement. The evolution was carried out over a finite interval of the flow parameter, sufficient for angular structure to evolve under the inverse mean curvature operator and for instabilities to emerge. Numerical diagnostics confirmed that for symmetric initial data the Hawking mass is preserved up to discretization error over this interval.

Although the evolution is restricted to a fixed spacelike hypersurface, the Hawking mass is computed using spacetime geometric quantities, allowing this flow to be interpreted as a hypersurface-restricted realization of a UEF. In selected runs, a small diffusion term was included in the evolution equation

$$\frac{\partial r}{\partial \lambda} = \frac{1}{H} + \eta\,\Delta_{S^2} r, \tag{18}$$

with $\eta \ll 1$, to suppress high-frequency numerical noise. Diagnostic quantities were monitored throughout the evolution to verify consistency of the scheme.

Angular dependence on the surface was discretized using a uniform grid in (θ, ϕ), with $\theta \in (0, \pi)$ and $\phi \in [0, 2\pi)$. Angular derivatives were computed using second-order finite-difference approximations in both angular directions, yielding a discrete representation of the spherical gradient and Laplacian operators. Spherical harmonic functions were used only for the specification of initial data and for diagnostic purposes, and not in the numerical evolution itself. The angular resolution was set by the number of grid points (N_θ, N_ϕ) and convergence was assessed by varying these parameters and verifying stability of the Hawking mass and other geometric quantities for both round and perturbed spheres.

Throughout the evolution, we monitor:

- the surface area $|\Sigma_\lambda|$,
- the integral $\int_{\Sigma_\lambda} H^2 \, dA$,
- the Hawking mass $m_H(\lambda)$,
- extrema of H over the surface.

4. Validation

Before studying surfaces under flow, we validate the numerical framework against geometries for which the Hawking mass and other relevant quantities are known analytically.

4.1. Round sphere in Minkowski spacetime

We first consider a round sphere of radius R embedded in a flat spacelike hypersurface of Minkowski spacetime. For this configuration, the Hawking mass vanishes identically. The numerical implementation reproduces the exact area, mean curvature, and Hawking mass to within discretization error. The results for the relevant geometric quantities are shown in Table 1. As a further consistency check, we computed m_H for varying mesh fineness, where N_θ and N_ϕ are the number of nodes in the θ and ϕ directions, respectively. The computed value converges to zero with second-order accuracy under angular mesh refinement (shown in Table 2). At our working resolution $N_\theta = 80$, $N_\phi = 160$, the residual numerical value is on the order of 7×10^{-5}, which we take to be the intrinsic discretization error.

Quantity	Computed Value	Expected Value
$\lvert\Sigma\rvert$	1.256471×10^1	1.256637×10^1
H	2.000000×10^0	2.000000×10^0
$\int H^2 \, \mathrm{d}A$	5.025886×10^1	5.026548×10^1
m_H	6.587962×10^{-5}	0

Table 1: Comparison of computed values for expected values for a round sphere in Minkowski spacetime.

N_θ	N_ϕ	m_H
32	64	4.277867×10^{-4}
64	128	1.035923×10^{-4}
80	160	6.5887962×10^{-5}
96	192	4.555647×10^{-5}

Table 2: Value for Hawking mass m_H for differing values of N_θ and N_ϕ.

4.2. Perturbed sphere in Minkowski spacetime

We next consider a small radial perturbation of the form

$$r(\theta, \phi) = R\,(1 + \varepsilon Y_{\ell m}(\theta, \phi))$$

and compute the Hawking mass without evolving the surface. We consider a single nontrivial spherical harmonic perturbation, choosing the axisymmetric mode Y_{20}. This provides a simple and representative deformation away from spherical symmetry while avoiding unnecessary mode coupling at the validation stage. For sufficiently small

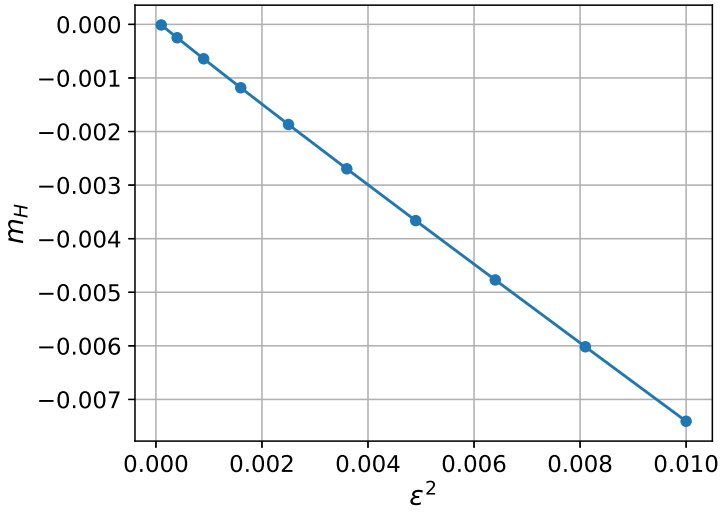


Figure 1: Hawking mass m_H of a perturbed sphere in Minkowski spacetime as a function of the perturbation amplitude squared ϵ^2. The linear scaling confirms the $\mathcal{O}(\epsilon^2)$ behaviour.

ε, the Hawking mass is expected to scale as $O(\varepsilon^2)$. This behavior is confirmed numerically, as shown in Fig. 1. The negative sign arises because small non-spherical perturbations of a round sphere in flat spacetime can lead to negative Hawking mass values, consistent with analytic expansions. We verified that the ϵ^2 scaling of m_H is robust under refinement of the angular mesh. Varying $N_\theta \in [32, 96]$ and $N_\phi \in [64, 192]$ as above, it was found that the Hawking mass changed by at most 7×10^{-5} for the largest value of ϵ and that the slope of m_H plotted against ϵ^2 remained unchanged.

5. Results

5.1. Flow on round sphere

As a consistency check, we evolved a round sphere in Minkowski spacetime under the in-slice flow. For this symmetric configuration, the Hawking mass vanishes identically and is expected to remain constant along the flow. Numerically, we compute the deviation $\Delta m_H(t) = m_H(t) - m_H(0)$ to isolate the accumulated error. Over the time interval used for the flow $\Delta m_H(t)$ remains small and exhibits no systematic drift, confirming that the numerical scheme preserves the Hawking mass for round spheres up to controlled numerical error (shown in Fig. 2). At the resolution we use, the maximum deviation remains at the level of 10^{-4}, consistent with the angular discretization and time-stepping errors discussed above.

5.2. Flow on a perturbed sphere

We finally move on to the case where the in-slice flow is performed for a perturbed sphere. To examine the influence of angular structure, we consider axisymmetric spherical harmonic perturbations of the round sphere (shown in Fig. 3). The $\ell = 2$ mode exhibits an approximately linear increase of m_H as a function of t, consistent with expectations from small perturbation analysis. Higher multipole perturbations ($\ell = 3, 4$) remain monotonic but display increased nonlinearity, reflecting the stronger contribution of angular derivatives to the evolution. This behavior is expected and does not indicate any loss of stability. To quantify monotonicity of the Hawking mass along the numerical flow, we define a discrete diagnostic δm_H

$$\delta m_H = \max_n \min(m_H(t_{n+1}) - m_H(t_n),\, 0)\,, \tag{19}$$

which measures the largest decrease of the Hawking mass between successive time steps. By construction, $\delta m_H = 0$ if and only if the discrete Hawking mass is monotonic non-decreasing along the flow.

This diagnostic was evaluated for initial data of the form $r(\theta, \phi) = R_0(1 + \epsilon\, Y_{20}(\theta, \phi))$ over a range of perturbation amplitudes $\epsilon \in [0.01, 0.07]$. For all values of ϵ considered, the diagnostic returned $\delta m_H = 0$ to machine precision, indicating that the Hawking mass remained monotonic throughout the discrete evolution. δm_H was also evaluated for initial data proportional to higher spherical harmonics $Y_{\ell 0}$ with $\ell = 3$ and $\ell = 4$.

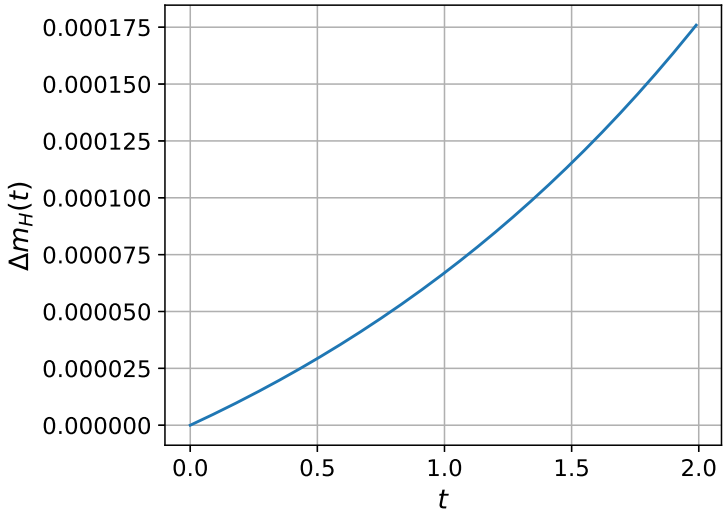


Figure 2: Deviation of the Hawking mass $\Delta m_H(t)$ for a round sphere evolved under the in-slice flow in Minkowski spacetime. Analytically, the Hawking mass of a round sphere vanishes and is preserved along the flow. The small nonzero deviation shown here is numerical and remains bounded throughout the evolution, indicating that the scheme preserves the expected invariance up to discretization error.

In all cases considered, δm_H remained zero to machine precision, indicating that the discrete Hawking mass is monotonic along the flow even in the presence of higher-frequency angular structure. This demonstrates robustness of the numerical scheme with respect to angular complexity of the initial surface. These results confirm that the in-slice, time-flat flow reproduces the monotonicity expected from the formal theory of UEFs for non-spherical surfaces in Minkowski spacetime.

We also explored initial data consisting of linear combinations of spherical harmonics. In contrast to the single mode evolutions discussed above, mixed mode perturbations exhibited increased sensitivity to numerical regularization, and the resulting Hawking mass evolution was not reliably monotonic within the present scheme. This behavior is consistent with the forward–backward parabolic character of the underlying flow and highlights the need for more refined numerical treatments or alternative formulations when strong mode coupling is present. In this work, we have therefore restricted the main analysis to single mode perturbations, for which the numerical behavior is robust.

6. Conclusions

In this work we have presented a numerical investigation of the Hawking mass under a restricted class of UEFs, realized in an in-slice, time-flat setting for tractability. Motivated by the formal monotonicity results of Bray-Hayward-Mars-Simon and Bray-Jauregui, the goal was to examine whether the monotonic behavior of the Hawking mass persists for non-spherical surfaces in a concrete computational setting [13, 14]. Using a discretized representation of perturbed spheres expanded in low-order spherical harmonics, we evolved single mode angular perturbations under an IMCF-type flow and tracked the resulting Hawking mass. After validating the numerical framework against analytic expectations for round and weakly perturbed spheres, we demonstrated that monotonicity of the Hawking mass is robust for a range of perturbation amplitudes and for multiple low-order spherical harmonics. These results provide explicit numerical evidence that the monotonicity mechanism underlying UEFs survives controlled departures from spherical symmetry.

Our study also highlights intrinsic limitations of the present approach. Evolutions involving mixed angular modes exhibited strong sensitivity to numerical regularization, reflecting the forward–backward parabolic character of the underlying flow equations. Similarly, extensions to spacetimes containing horizons or to fully spacetime-based UEFs introduce additional geometric and numerical challenges which are beyond the scope of the present work. These observations suggest that more sophisticated formulations or regularization strategies will be required to extend this analysis to multi-mode interactions and black hole spacetimes. Despite these limitations, the results presented here constitute, to our knowledge, the first systematic numerical exploration of evolution of the Hawking mass under UEFs for non-spherical surfaces (in this case, the UEF was slice-restricted

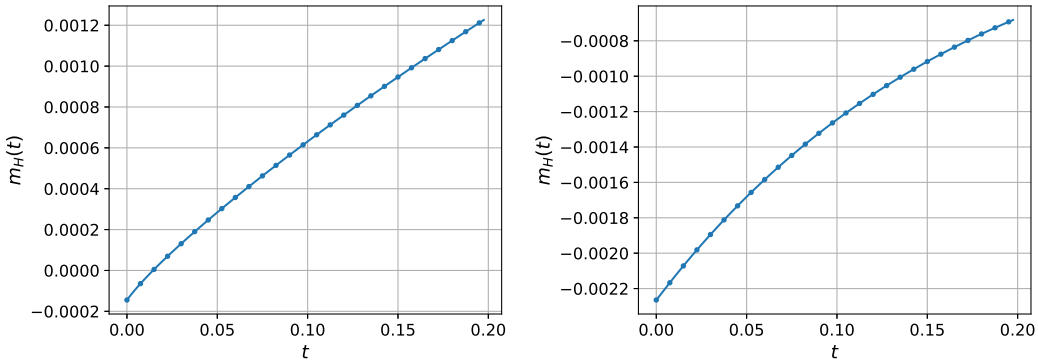


Figure 3: Evolution of the Hawking mass under in-slice flow for a perturbed sphere. Shown are the results for (left) Y_{20} and (right) Y_{30}, with $\epsilon = 0.05$ in both cases. The Hawking mass evolves monotonically for both harmonics, although higher multipole structure leads to increased curvature in the mass–time relation due to stronger angular gradients, reflecting the larger contribution of angular derivatives to the evolution in higher- ℓ modes. No numerical instabilities or violations of monotonic behavior are observed.

and time-flat for numerical tractability). This approach supplies physics-level evidence that the monotonicity persists beyond the formal idealized setting and offers insight into the robustness of uniformly expanding flows as a tool for quasi-local energy diagnostics. It also complements existing formal results and offers a starting point for further numerical studies of quasi-local mass and geometric flows, as well as their role in gravitational physics.

Acknowledgments

The author thanks Béatrice Bonga for useful discussions. This research was conducted whilst the author was visiting the Okinawa Institute of Science and Technology (OIST) through the Theoretical Sciences Visiting Program (TSVP).

Data availability

The numerical codes used to generate the results presented in this article are available at `https://github.com/Tom467/HawkingmassUEFs`. No experimental data were generated or analysed during the current study.

Conflict of Interest

The authors have no conflicts to disclose.

References

[1] A.J. Dougan and L.J. Mason, Quasilocal mass constructions with positive energy, Phys. Rev. Lett. **67**, 2119-2122 (1991).
[2] L.B. Szabados, On the positivity of the quasi-local mass (general relativity), Class. Quantum Grav. **10**, 1899 (1993).
[3] J. David Brown and J.W. York, Jr., Quasilocal energy and conserved charges derived from the gravitational action, Phys. Rev. D **47**, 1407 (1993).
[4] M.-T. Wang and S.-T. Yau, Quasilocal Mass in General Relativity, Phys. Rev. Lett. **102**, 021101 (2009).
[5] L.B. Szabados, Quasi-local energy-momentum and angular momentum in general relativity, Living Rev. Relativ. **12**, 4 (2009).
[6] N.Ó. Murchadha, L.B. Szabados and K.P. Tod, Comment on "Positivity of quasilocal mass", Phys. Rev. Lett. **92**, 259001 (2004).
[7] C.-C.M. Liu and S.-T. Yau, Positivity of quasilocal mass, Phys. Rev. Lett. **90**, 231102 (2003).
[8] S.W. Hawking, Gravitational Radiation in an Expanding Universe, J. Math. Phys. **9**(4), 598-604 (1968).
[9] R. Penrose, Naked singularities, Ann. N.Y. Acad. Sci. **224**, 125 (1973).
[10] M. Mars, Present status of the Penrose inequality, Class. Quantum Grav. **26**, 193001 (2009).
[11] G. Huisken and T. Ilmanen, The inverse mean curvature flow and the Riemannian Penrose inequality, J. Differ. Geom. **59**, 353 (2001).
[12] H.L. Bray, Proof of the Riemannian Penrose inequality using the positive mass theorem, J. Differ. Geom. **59**, 177 (2001).
[13] H. Bray, S. Hayward, M. Mars and W. Simon, Generalized Inverse Mean Curvature Flows in Spacetime, Commun. Math. Phys. **272**, 119-138 (2007).

[14] H.L. Bray and J.L. Jauregui, Time Flat Surfaces and the Monotonicity of the Spacetime Hawking Mass, Commun. Math. Phys. **335**, 285-307 (2015).
[15] E. Witten, A new proof of the positive energy theorem, Commun. Math. Phys. **80**, 381–402 (1981).
[16] T. Parker and C.H. Taubes, On Witten's proof of the positive energy theorem, Commun. Math. Phys. **84**, 223 (1982).
[17] R. Geroch, Energy extraction, Ann. N.Y. Acad. Sci. **224**, 108 (1973).
R. Geroch, General relativity, Proc. Symp. Pure Math. **27**, 401 (1975).
[18] Y. Choquet-Bruhat and J. Marsden, Sur la positivité de la masse, C.R. Acad. Sci. **282**, 609 (1976).
Y. Choquet-Bruhat and J. Marsden, Solution of the local mass problem in general relativity, Commun. Math. Phys. **51**, 283 (1976).
[19] P. Grandclément and J. Novak, Spectral Methods for Numerical Relativity, Living Rev. Reativ. **12**, 1 (2009).
[20] N.T. Bishop and L. Rezzolla, Extraction of gravitational waves in numerical relativity, Living Rev. Relativ. **19**, 2 (2016).
[21] K.D. Kokkotas and B.G. Schmidt, Quasi-normal modes of stars and black holes, Liv. Rev. Relativ. **2**, 2 (1999).
[22] L. Motl, An analytical computation of asymptotic Schwarzschild quasinormal frequencies, Adv. Theor. Math. Phys. **6**, 1135-1162 (2002).
[23] L. Motl and A. Neitzke, Asymptotic black hole quasinormal frequencies, Adv. Theor. Math. Phys. **7**, 307-330 (2003).
[24] A.K.-W. Chung, P. Wagle and N. Yunes, Spectral method for the gravitational perturbations of black holes: Schwarzschild background case, Phys. Rev. D **107**, 124032 (2023).